Check for updates

View Article Online
View Journal

Chemical
Science

Accepted Manuscript

This article can be cited before page numbers have been issued, to do this please use: M. An, C. Lu, F. Xie, Y. Sun, Z. Sun, L. Xi and R. Liu, *Chem. Sci.*, 2026, DOI: 10.1039/D6SC03274E.

Chemical
Science
Volume 9
Number 1
7 January 2018
Pages 1-268
rsc.li/chemical-science
ISSN 2041-6539
ROYAL SOCIETY OF CHEMISTRY
EDGE ARTICLE
Xinjing Tang *et al.*
Caged circular siRNAs for photomodulation of gene expression in cells and mice

This is an Accepted Manuscript, which has been through the Royal Society of Chemistry peer review process and has been accepted for publication.

Accepted Manuscripts are published online shortly after acceptance, before technical editing, formatting and proof reading. Using this free service, authors can make their results available to the community, in citable form, before we publish the edited article. We will replace this Accepted Manuscript with the edited and formatted Advance Article as soon as it is available.

You can find more information about Accepted Manuscripts in the Information for Authors.

Please note that technical editing may introduce minor changes to the text and/or graphics, which may alter content. The journal's standard Terms & Conditions and the Ethical guidelines still apply. In no event shall the Royal Society of Chemistry be held responsible for any errors or omissions in this Accepted Manuscript or any consequences arising from the use of any information it contains.

ROYAL SOCIETY
OF CHEMISTRY

rsc.li/chemical-science

View Article Online
DOI: 10.1039/D6SC03274E

Organocatalytic Asymmetric Synthesis of Atropisomeric Tetraarylethenes: Design, Properties, and Applications

Mei An,†[a,b] Chuan-Jun Lu,†[b] Fei Xie,[b] Yin-Jian Sun,[b] Zhaofeng Sun,[c] Long-Long Xi*[b] and Ren-Rong Liu*[a,b]

Received 00th January 20xx,
Accepted 00th January 20xx

DOI: 10.1039/x0xx00000x

rsc.li/chemical-science

Tetraarylethenes are important π-conjugated molecules with versatile applications in OLEDs, fluorescent probes, and aggregation-induced emission (AIE) luminogens. Access to chiral TAEs is largely limited to strategies relying on preinstalled chiral elements or post-synthetic resolution, restricting structural diversity and functional exploration. Herein, we report a CPA-catalysed atroposelective transfer hydrogenation enabling the direct construction of axially chiral TAEs via desymmetrization of TAE dialdehydes with anilines. This method features broad substrate scope, excellent enantioselectivity, and remarkable AIE properties. Our work provides a practical catalytic approach to access structurally diverse chiral TAEs, offering new opportunities for the development of functional chiral luminogens and optoelectronic materials.

Introduction

Tetraarylethenes (TAEs) represent an important class of π-conjugated organic molecules characterized by a central C=C double bond bearing four aryl substituents. Owing to their rigid conjugated frameworks, structural tunability, and distinctive electronic properties, TAEs have garnered significant attention in both material science, bio-sensors, and organic synthesis.[1] They serve as versatile building blocks for functional materials, including metal organic frameworks,[2] fluorescent probes,[3] and aggregation-induced emission (AIE) luminogens (Scheme 1A).[4] In addition, their unique photophysical behavior enables diverse applications in molecular switches,[5] molecular recognition,[6] and circularly polarized luminescence (CPL).[7] Consequently, the development of efficient and general synthetic strategies to access structurally diverse and chiral TAEs is of great significance for advancing both fundamental studies and practical applications.

Traditional approaches to access optically active TAEs typically rely on the incorporation of external chiral auxiliaries or chiral side chains into the TAE framework, thereby introducing central or axial chirality (Scheme 1B).[8] Another widely employed strategy involves exploiting helical chirality; for instance, Zheng and co-workers achieved the resolution of racemic hindered tetraphenylethylene helicates through chiral chromatography.[9] These chiral TAEs exhibited remarkable AIE characteristics, along with notable chiral recognition and CPL properties. Despite these advances, the synthesis of chiral TAEs remains largely dependent on preinstalled chiral elements or post-synthetic resolution, which restricts structural diversity and limits further exploration of their functional potential. The lack of efficient catalytic systems capable of directly inducing chirality within the TAE core has significantly hindered the development of new chiral architectures and the in-depth study of their optoelectronic and supramolecular behaviors. Recently, Tan and co-workers reported the first CPA-catalysed enantioselective synthesis of TAEs via an electrophilic aromatic substitution-enabled desymmetrization of prochiral substrates.[10] Nevertheless, catalytic asymmetric strategies that enable the direct construction of chiral TAEs remain in their infancy and are urgently needed to expand the accessible chemical space of these chiral luminogens.

Chiral phosphoric acids[11] have proven to be highly effective catalysts in asymmetric transfer hydrogenation (ATH) reactions of α, β-unsaturated carbonyls, imines, and heterocycles, typically employing Hantzsch esters or benzothiazolines as hydrogen donors.[12] Notably, substantial progress has been achieved in CPA- and enzyme-catalysed atroposelective transfer hydrogenations for the construction of axially chiral biaryls.[13] In parallel, remarkable advances have also been made in the asymmetric catalytic synthesis of axially chiral aryl-alkenes over the past few years.[14] Inspired by these precedents, we envisioned that axially chiral TAEs could be accessed via a desymmetrization strategy involving the condensation of TAE dialdehydes with anilines under CPA-catalysed asymmetric transfer hydrogenation. Herein, we disclose the first example of a CPA-catalysed atroposelective transfer hydrogenation enabling the direct construction of axially chiral TAEs (Scheme 1C). This method features mild reaction conditions, a broad substrate scope, and remarkable enantioselective control. Moreover, the resulting products exhibit excellent AIE characteristics.

---

[a] College of Pharmaceutical Sciences, Guizhou University, Guiyang, Guizhou 550025, China. E-mail: renrongliu@qdu.edu.cn
[b] College of Chemistry and Chemical Engineering, Qingdao University, Qingdao 266071, China. E-mail: xill@qdu.edu.cn
[c] School of Rehabilitation Sciences and Engineering, University of Health and Rehabilitation Sciences, Qingdao 266113, China

† These authors contributed equally.

View Article Online
DOI: 10.1039/D6SC03274E

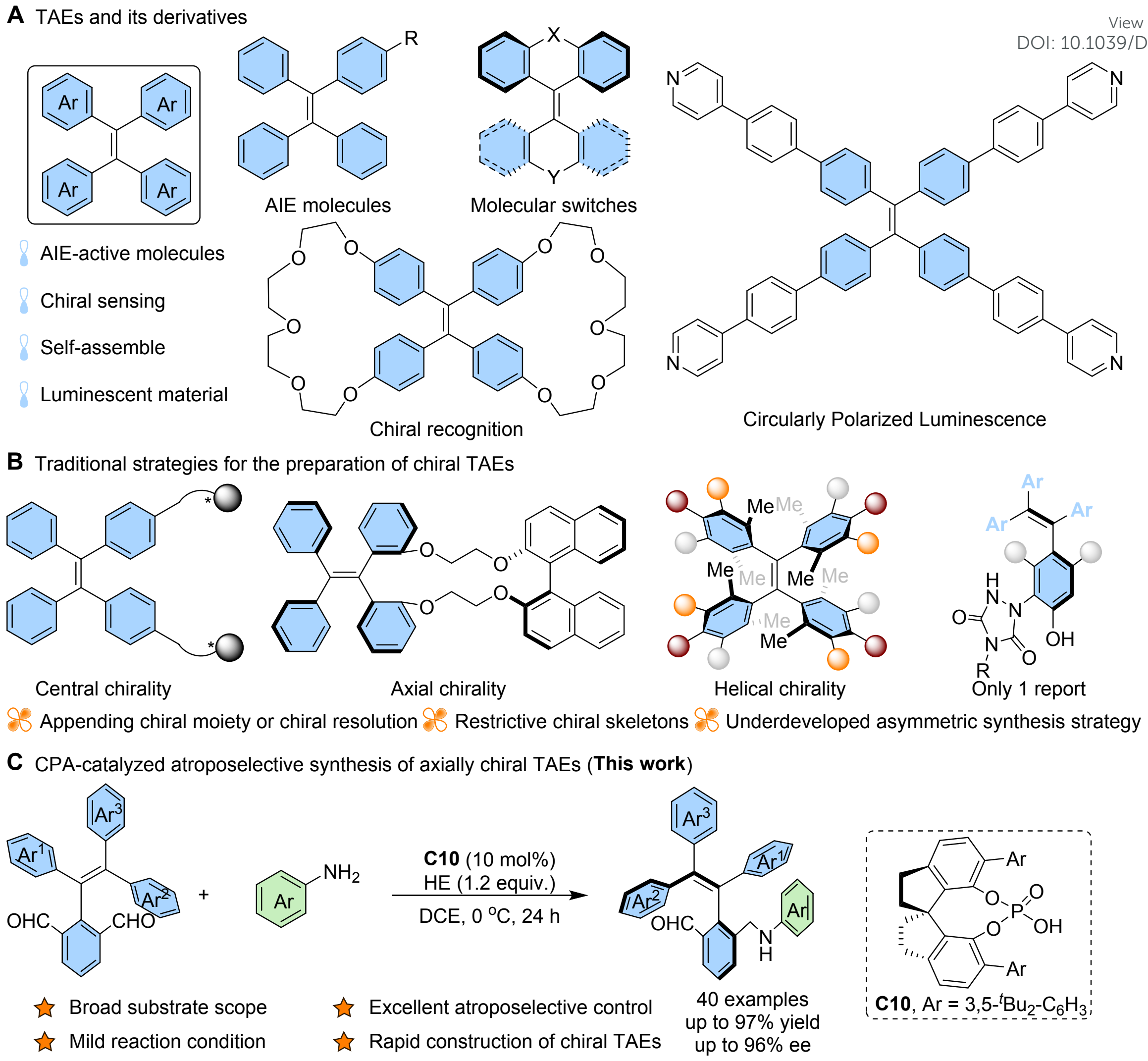

Scheme 1 Applications of chiral TAEs and our reaction design.

Results and discussion

Reaction condition optimization

To gain initial insights into the reaction parameters, we selected TAE dialdehyde **1a** and 4-methoxyaniline **2a** as model substrates to investigate the reaction under atroposelective transfer hydrogenation conditions, using the Hantzsch ester as the hydrogen source and a chiral phosphoric acid (CPA) as the catalyst (Table 1). Under the preliminary conditions (**C1**, 10 mol% in toluene at room temperature for 12 h), the desired product **3a** was obtained in 63% yield with a modest enantioselectivity 11% ee (Table 1, entry 1). Next, a series of chiral BINOL-derived CPAs **C2**-**C6** were evaluated (entries 2-6), among which catalyst **C4** bearing bulky aryl substituents afforded the best enantioselectivity of 59% ee (entry 4). To further enhance the asymmetric induction, various axially chiral backbones of CPAs were then examined (entries 7-11). Notably, the 1,1′-spirobiindane-diol-derived **C10** exhibited superior catalytic performance, affording the desired product **3a** in 70% yield with 80% ee (entry 10). Subsequent solvent screening showed that DCE was the most effective medium for enantiocontrol among CCl_4, DCM, and DCE (entries 12-14), affording **3a** in 70% yield and an excellent 91% ee (entry 14). Lowering the temperature to 0 °C further improved the enantioselectivity to 93% (entry 15). Finally, extending the reaction time to 24 h led to a slightly higher isolated yield (72%) while maintaining the same excellent enantioselectivity (entry 16). Notably, the bis-reductive amination byproduct arising from a second reductive amination of **3a** was consistently detected during reaction optimization. When the loading of catalyst **C10** was reduced to 5 mol%, product **3a** was obtained in only 53% yield with a decreased ee of 91% (entry 17).

Substrate scope

With the optimized reaction conditions in hand, we next explored the substrate scope of the CPA-catalysed atroposelective transfer hydrogenation using TAE dialdehyde **1a** as the standard substrate (Table 2). A diverse array of aromatic amines **2** bearing various electronic and steric features were examined to evaluate the generality of this transformation. Anilines containing electron-donating substituents such as alkoxy (**2a**-**2c**), methyl (**2d**), or aryl (**2e**-**2f**) groups underwent smooth conversion to the corresponding

View Article Online
DOI: 10.1039/D6SC03274E

Table 1 Optimization of the reaction conditions

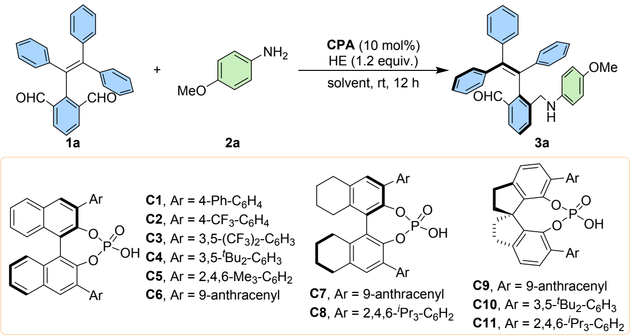

Entry	**CPA** (10 mol%)	Solvent	T (°C)	Time	Yield of **3a** (%)[a]	Ee of **3a** (%)[b]
1	**C1**	Toluene	25	12 h	63	11
2	**C2**	Toluene	25	12 h	55	27
3	**C3**	Toluene	25	12 h	40	7
4	**C4**	Toluene	25	12 h	65	59
5	**C5**	Toluene	25	12 h	63	29
6	**C6**	Toluene	25	12 h	65	57
7	**C7**	Toluene	25	12 h	50	53
8	**C8**	Toluene	25	12 h	46	3
9	**C9**	Toluene	25	12 h	72	75
10	**C10**	Toluene	25	12 h	70	80
11	**C10**	Toluene	25	12 h	55	63
12	**C10**	CCl_4	25	12 h	75	85
13	**C10**	DCM	25	12 h	62	89
14	**C10**	DCE	25	12 h	70	91
15	**C10**	DCE	0	12 h	58	93
16	**C10**	DCE	0	24 h	78(72)[c]	93
17[d]	**C10**	DCE	0	24 h	53	91

Unless otherwise specified, the reaction conditions were as follows: **1a** (0.10 mmol), **2a** (0.10 mmol), 10 mol% CPA, and 1.2 equiv. of HE in 1.0 mL of solvent at 0-25 °C for 12-24 h. [a]Determined by ^{1}H-NMR analysis. [b]Determined by chiral HPLC analysis. [c]Isolated yield in the parentheses. [d]5 mol% **C10**.

axially chiral products **3a**-**3f** in good to excellent yields (65-81%) and high enantioselectivities (89-93% ee). Similarly, *para*-halogenated anilines (F, Cl, Br) were well tolerated, delivering the desired products **3g**-**3i** with excellent enantioselectivities. The absolute configuration of this class of products was unambiguously determined to be *S* by single-crystal X-ray diffraction analysis of compound **3i** (CCDC 2494773), thereby establishing the stereochemical correlation for this series. Anilines bearing polar or functionalized substituents such as phenolic hydroxyl, benzoyl, or pyrrolyl groups were also compatible, affording the corresponding products **3j**-**3l** in moderate yields with good enantioselective control. Furthermore, disubstituted anilines with 3,4- or 3,5-methyl/methoxy patterns smoothly furnished the products **3m**-**3p** in up to 80% yield and 93% ee, demonstrating that sterically encumbered substrates are also well accommodated. Notably, *ortho*-substituted 3-amino-4-methylphenol gave the product **3q** in slightly reduced yield but maintained excellent enantioselectivity, indicating that steric hindrance near the reaction site primarily affects the reactivity rather than the asymmetric induction. Moreover, anilines containing 3,4,5-trisubstitution patterns were also suitable, affording **3r** with good efficiency. The reaction proved to be highly general, extending to aromatic amines bearing naphthyl, anthracenyl, and heteroaromatic moieties, which furnished the corresponding products **3s**-**3ab** in moderate yields and high enantioselectivities (83-93% ee). We experimentally determined the rotational barrier of **3ab** to be 33.2 kcal/mol at 140 °C in mesitylene. Finally, to demonstrate the synthetic versatility of this methodology, we extended the reaction to structurally complex anilines bearing secondary alkylamine or lactam substituents at the *para*-position. Both substrates underwent smooth transformation to afford the corresponding axially chiral TAE derivatives **3ac**-**3ae** in good yields with excellent enantioselectivities or diastereoselectivity (> 20:1 dr), underscoring the robustness and broad applicability of this asymmetric transformation for the late-stage modification of complex molecules.

The substrate scope was next explored using a series of TAE dialdehydes **1** and 4-methoxyaniline **2a** as the model substrate (Table 3). We first examined TAEs bearing *para*-substituents on the aryl rings at the distal position of the benzaldehyde moiety. Methyl, and halogen groups were all well tolerated, affording the corresponding products **4a**-**4c** in 52-68% yields with 81-96% ee. Notably, the fluorene-substituted TAE also performed well under the standard conditions, delivering **4d** in 63% yield and 91% ee. Subsequently, TAEs bearing *para*- or *meta*-substituents on the aryl ring directly attached to the same carbon center as the benzaldehyde were also evaluated, furnishing the desired axially chiral TAEs **4e**-**4h** in 62-88% yields with good enantioselectivities (90-91%). Moreover, excellent enantioselectivity was achieved in the reaction of an unsymmetrical TAE (*Z*/*E* = 1/1) with **2a**, affording **4i** (*Z*/*E* = 1/1) in 71% yield.

Table 2 Reaction scope of aromatic amines

View Article Online
DOI: 10.1039/D6SC03274E

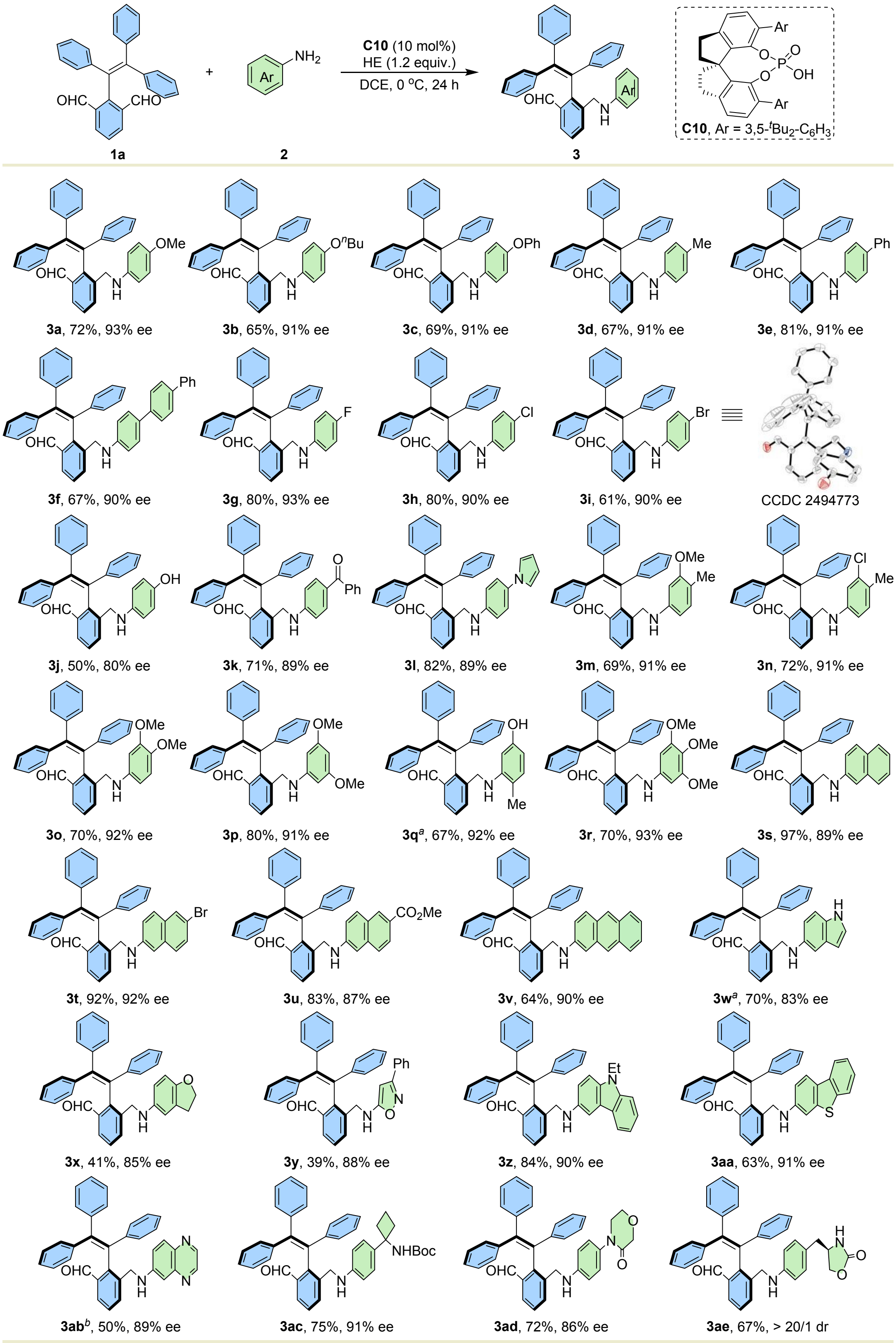

Reaction conditions: **1a** (0.10 mmol), **2** (0.10 mmol), 10 mol% CPA, and 1.2 equiv. of HE in 1.0 mL of DCE at 0 °C for 24 h; isolated yield by silica gel chromatography; ee values were determined by chiral HPLC. [a]72 h. [b]-10 °C, 72 h.

View Article Online
DOI: 10.1039/D6SC03274E

Table 3 Reaction scope of TAE dialdehydes

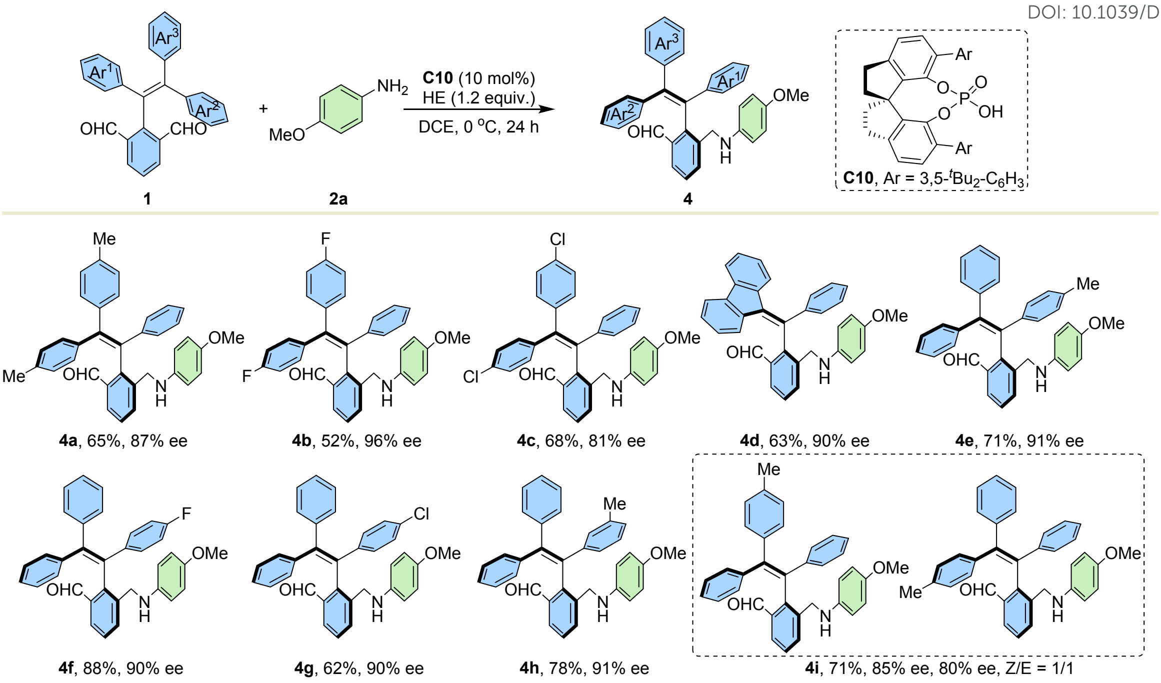

Reaction conditions: **1** (0.10 mmol), **2a** (0.10 mmol), 10 mol% CPA, and 1.2 equiv. of HE in 1.0 mL of DCE at 0 °C for 24 h; isolated yield by silica gel chromatography; ee values were determined by chiral HPLC.

Synthetic applications and mechanistic studies

To further demonstrate the practicality and scalability of this atroposelective strategy for constructing axially chiral TAEs, a large-scale reaction was carried out (Scheme 2A). The reaction between TAE dialdehyde **1a** and *p*-toluidine **2d** on a 2.0 mmol scale proceeded smoothly under the standard conditions, affording product **3d** in 75% yield while maintaining its high enantioselectivity. Subsequently, a series of derivatization transformations of **3d** was conducted to showcase the synthetic versatility of this method (Scheme 2B). Reduction of the aldehyde moiety with $NaBH_4$ furnished benzyl alcohol **5a** in 61% yield without any loss of enantioselectivity. Protection of the N–H group in **3d** with TsCl afforded sulfonamide **5b** in moderate yield, with only a slight decrease in enantiopurity. Condensation of the aldehyde with hydroxylamine hydrochloride and *R*-tert-butylsulfinamide produced oxime **5c** and sulfinamide **5d** in high yields (56-72%) with excellent enantioselectivity (91% ee) or diastereoselectivity (> 20:1 dr), respectively. Moreover, **3d** could undergo further reductive amination to afford **5e** in 46% yield, albeit with a slight decrease in enantiomeric excess. To evaluate the configurational stability of these axially chiral TAEs, racemization experiments were performed on **3p**, revealing a rotational barrier of 33.8 kcal/mol at 120 °C in toluene (Scheme 2C), indicating that this class of compounds is configurationally stable at room temperature and does not readily undergo racemization under reaction conditions. Subsequently, non-linear effect studies exhibited a linear correlation between the ee of product **3p** and that of catalyst **C10**, suggesting that a monomeric catalyst species is involved in the enantio-determining transition state (Scheme 2D). Finally, control experiments were conducted to probe the reaction mechanism (Scheme 2E). Under the standard conditions but in the absence of the Hantzsch ester, the reaction between **1a** and **2a** afforded the corresponding imine **3a′** in 63% yield as a racemate. In addition, treatment of *rac*-**3d** with **2p** under the standard conditions delivered enantioenriched **3d** in 27% yield with 87% ee, together with **ent-5e** in 60% yield and 60% ee (Scheme 2F). These results suggest that stereocontrol is established during the CPA-catalyzed ATH reduction of the imine intermediate, while a subsequent kinetic resolution process further enhances the enantioselectivity.

View Article Online
DOI: 10.1039/D6SC03274E

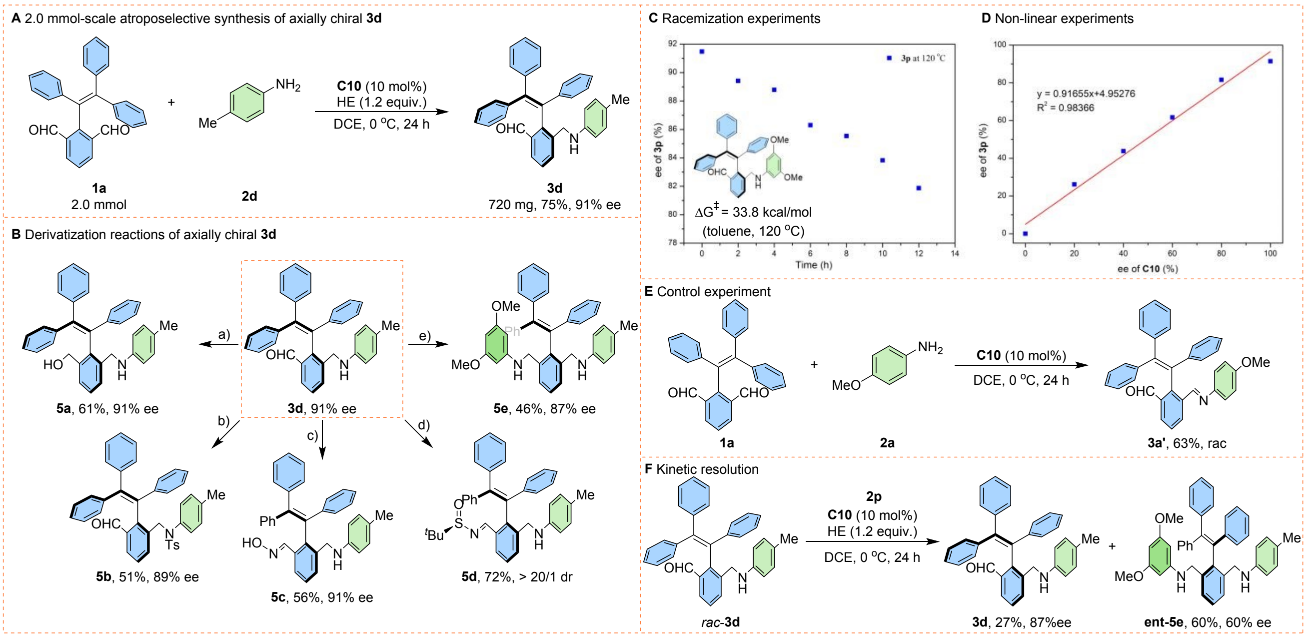

Scheme 2 Synthetic applications and mechanistic studies. Reaction conditions: a) $NaBH_4$ (1.2 equiv.), THF/H_2O (4/1), 0 °C, 2 h; b) TsCl (1.5 equiv.), Et_3N (3.0 equiv.), DMAP (10 mol%), DCM, 0 °C to rt, 12 h; c) $NH_2OH{\cdot}HCl$ (1.2 equiv.), NaOAc (1.2 equiv.), MeOH/H_2O (9/1), rt, 5 min; d) (R)-^{t}BuSA (3.0 equiv), $Ti(OEt)_4$ (3.0 equiv.), DCM, 50 °C, 12 h; e) **2p** (1.0 equiv.), $(PhO)_2PO_2H$ (10 mol%), HE (1.0 equiv.), Et_2O, rt, 1 h.

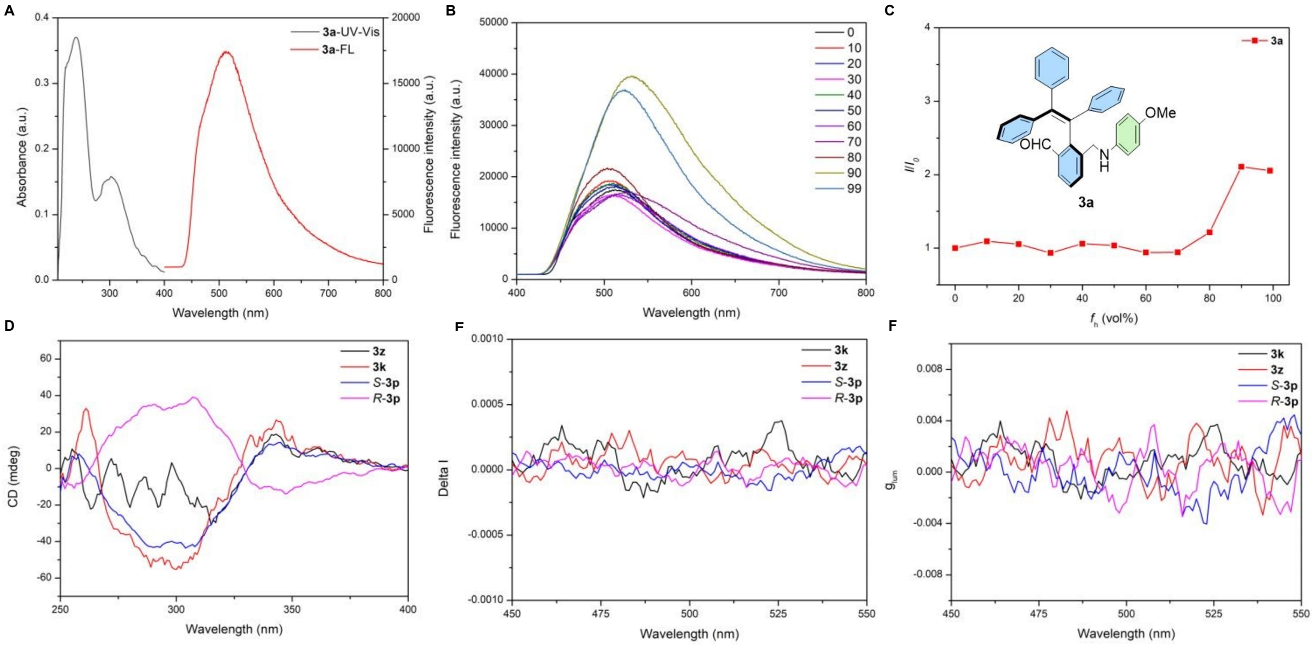

Fig. 1 Photophysical and optical property investigations

Optical property investigation

A comprehensive investigation of the photophysical characteristics of selected axially chiral TAEs was carried out (Fig. 1). In the UV-vis spectra, an intense absorption feature appeared near 240 nm, accompanied by weaker transitions around 305 nm (Fig. 1A). Upon photoexcitation at 340 nm, the compounds emitted fluorescence centered at approximately 510 nm. Moreover, the AIE properties of the newly developed axially chiral TAE framework were evaluated

View Article Online
DOI: 10.1039/D6SC03274E

(Fig. 1B, C). Compound **3a** exhibited only weak fluorescence in THF/H_2O mixtures when the water fraction (*f*⍰) was below 80%. As *f*⍰ increased, the emission intensity gradually intensified. Notably, when *f*⍰ > 90%, a distinct fluorescence band appeared at 530 nm, clearly confirming the pronounced AIE behavior of these chiral TAE derivatives. The CD spectra of the two enantiomers, *S*-**3p** and *R*-**3p**, exhibited mirror-image Cotton effects (Fig. 1D), demonstrating that the chiral integrity of the molecules was well preserved; in all cases, the S-isomers consistently showed positive Cotton responses. CPL measurements revealed distinct emission activity for **3k**, **3z**, *S*-**3p**, and *R*-**3p** (Fig. 1E), with their corresponding luminescence dissymmetry factors ($|g_{lum}|$) determined from the emission profiles (Fig. 1F). Among these, compound **3z** displayed the highest $|g_{lum}|$ value of 0.00222, underscoring its promise as a potential CPL-active material for optoelectronic applications.

Conclusions

In summary, we have developed a highly efficient CPA-catalysed atroposelective transfer hydrogenation for the direct construction of axially chiral TAEs. This method features broad substrate scope, excellent enantioselective control, and scalability. The resulting chiral TAEs exhibit remarkable optical and potential AIE properties, highlighting their potential in optoelectronic and chiroptical applications. Further exploration of the AIE mechanism and structure-property relationship is currently ongoing in our laboratory.

Author contributions

M. A., C.-J. L., F. X., Y.-J. S., and Z.S. performed the experiments. All authors contributed to analysing the experimental resulted. R.-R. L. and L.X. conceived the study, supervised the project, and wrote the paper.

Conflicts of interest

There are no conflicts to declare

Data availability

The data supporting this article have been included as partof the supplementary information (SI).

CCDC 2494773 contains the supplementary crystallographicdata for this paper.

Acknowledgements

This work was supported by the National Natural Science Foundation of China (22371152, 22501151), and National Natural Science Foundation of Shandong (ZR2023JQ006, ZR2024QB091).

Notes and references

1. (a) R. Hu, N. L. C. Leung and B. Z. Tang, *Chem. Soc. Rev*., 2014, **43**, 4494–4562; (b) H.-T. Feng, Y.-X. Yuan, J.-B. Xiong, Y.-S. Zheng and B. Z. Tang, *Chem. Soc. Rev*., 2018, **47**, 7452–7476; (c) G. Feng and B. Liu, *Acc. Chem. Res*., 2018, **51**, 1404–1414; (d) R. S. Bhosale, M. Aljabri, D. D. La, S. V. Bhosale, L. A. Jones and S. V. Bhosale, *Cham*., 2019, 223–264; (e) D. Dai, J. Yang and Y.-W. Yang, *Chem. Eur. J*., 2022, **28**, e202103185; (f) D.-M. Li, R. Zuo, J. Wang and Z. Le, *Chem. Eur. J*., 2025, **31**, e202403715.
2. (a) N. B. Shustova, B. D. McCarthy and M. Dincă, *J. Am. Chem. Soc*., 2011, **133**, 20126–20129; (b) N. B. Shustova, T.-C. Ong, A. F. Cozzolino, V. K. Michaelis, R. G. Griffin and M. Dincă, *J. Am. Chem. Soc*., 2012, **134**, 15061–15070; (c) Z. Wei, Z.-Y. Gu, R. K. Arvapally, Y.-P. Chen, R. N. McDougald, Jr, J. F. Ivy, A. A. Yakovenko, D. Feng, M. A. Omary, H.-C. Zhou, *J. Am. Chem. Soc*., 2014, **136**, 8269–8276.
3. (a) J. Wu, W. Liu, J. Ge, H. Zhang and P. Wang, *Chem. Soc. Rev*., 2011, **40**, 3483–3495; (b) R. T. Kwok, C. W. Leung, J. W. Lam and B. Z. Tang, *Chem. Soc. Rev*., 2015, **44**, 4228–4238; (c) X.-Y. Lou and Y.-W. Yang, *Adv. Optical Mater*., 2018, **6**, 1800668; (d) Y. L. Balachandran and X. Jiang, *CCS Chem*., 2022, **4**, 420–436.
4. (a) D. Ding, K. Li, B. Liu and B. Z. Tang, *Acc. Chem. Res*., 2013, **46**, 2441–2453; (b) J. Mei, N. L. C. Leung, R. T. K. Kwok, J. W. Y. Lam and B. Z. Tang, *Chem. Rev*., 2015, **115**, 11718–11940; (c) H. Wang et al. *ACS Nano*., 2023, **17**, 14347–14405.
5. (a) R. Hein, C. N. Stindt and B. L. Feringa, *J. Am. Chem. Soc*., 2024, **146**, 26275–26285; (b) R. Hein, Y. Gisbert and B. L. Feringa, *J. Am. Chem. Soc*., 2025, **147**, 13649–13657.
6. X. Tian, M. Zuo, Y. Shen, N. Mao, K. Wang, Y. Sheng, K. Velmurugan, Ji. Jiao and X.-Y. Hu, *Nat. Commun*., 2024, **15**, 7182.
7. M. Lu, P. Li, X. Dong, Z. Jiang, S. Ren, J. Yao, H. Dong and Y. S. Zhao, *Angew. Chem. Int. Ed*., 2024, **63**, e202408619.
8. (a) H. Li, J. Cheng, Y. Zhao, J. W. Y. Lam, K. S. Wong, H. Wu, B. S. Li and B. Z. Tang, *Mater. Horiz*., 2014, **1**, 518–521; (b) H.-T. Feng, X. Zhang and Y.-S. Zheng, *J. Org. Chem*., 2015, **80**, 8096–8101; (c) H.-T. Feng, C. L, Q. Li, H. Zhang, J. W. Y. Lam and B. Z. Tang, *ACS Materials Lett*. 2019, **1**, 192–202; (d) M. Hu, Y.-X. Yuan, W. Wang, D.-M. Li, H.-C. Zhang, B.-X. Wu, M. Liu and Y.-S. Zheng, *Nat. Commun*., 2020, **11**, 161.
9. (a) J.-B. Xiong, H.-T. Feng, J.-P. Sun, W.-Z. Xie, D. Yang, M. Liu and Y.-S. Zheng, *J. Am. Chem. Soc*., 2016, **138**, 11469–11472; (b) M. Hu, F.-Y. Ye, C. Du, W. Wang, W. Yu, M. Liu and Y.-S. Zheng, *Angew. Chem. Int. Ed*., 2022, **61**, e202115216; (c) W. Yu, M. Hu, Z.-R. Xu, J.-J. Fu and Y.-S. Zheng, *Org. Lett*., 2025, **27**, 1256–1260.
10. W. Bao, S.-Q. Qiu, S.-H. Wang, H.-H. Liu, S.-H. Xiang and B. Tan, *Angew. Chem. Int. Ed*., 2025, **64**, e202519340.
11. (a) T. Akiyama, Chem. Rev., 2007, **107**, 5744–5758; (b) D. Parmar, E. Sugiono, S. Raja and M. Rueping, *Chem. Rev*., 2017, **117**, 10608 – 10620; (c) R. Maji, S. C. Mallojjala and S. E. Wheeler, *Chem. Soc. Rev*., 2018, **47**, 1142–1158; (d) Z.-L. Xia, Q.-F. Xu, C. Zheng and S.-L. You, *Chem. Soc. Rev*., 2020, **49**, 286–300; (e) B.-C. Da, S.-H. Xiang, S. Li and B. Tan, *Chin. J. Chem*., 2021, **39**, 1787–1796; (f) J. K. Cheng, S.-H. Xiang, S. Li, L. Ye and B. Tan, *Chem. Rev*., 2021, **121**, 4805–4902; (g) J. K. Cheng, S.-H. Xiang, B. Tan, *Acc. Chem. Res*., 2022, **55**, 2920–2937.

12. (a) Q.-A. Chen, M.-W. Chen, C.-B. Yu, L. Shi, D.-S. Wang, Y. Yang and Y.-G. Zhou, *J. Am. Chem. Soc.*, 2011, **133**, 16432–16435; (b) C. Zheng and S.-L. You, *Chem. Soc. Rev.*, 2012, **41**, 2498–2518; (c) D. Wang and D. Astruc, *Chem. Rev.*, 2015, **115**, 6621–6686; (d) J. Zhang and J. Wang, *Angew. Chem. Int. Ed.*, 2018, **57**, 465–469; (e) Y. Gao, G. Hong, B.-M. Yang and Y. Zhao, *Chem. Soc., Rev.*, 2023, **52**, 5541–5562; (f) M.-W. Chen, B. Wu, Z. Liu and Y.-G. Zhou, *Acc. Chem. Res.*, 2023, **56**, 2096–2109.
13. (a) D.-J. Cheng, L. Yan, S.-K. Tian, M.-Y. Wu, L.-X. Wang, Z.-L. Fan, S.-C. Zheng, X.-Y. Liu and B. Tan, *Angew. Chem. Int. Ed.*, 2014, **53**, 3684–3687; (b) K. Mori, T. Itakura and T. Akiyama, *Angew. Chem. Int. Ed.*, 2016, **55**, 11642–11646; (c) Y.-D. Shao, J.-S. Feng, D.-D. Han, K.-H. Pan, L. Zhang, Y.-F. Wang, Z.-H. Ma, P.-R. Wang, M.-J. Yin and D.-J. Cheng, *Org. Chem. Front.*, 2022, **9**, 764–770; (d) L. Dai, Y. Liu, Q. Xu, M. Wang, Q. Zhu, P. Yu, G. Zhong and X. Zeng, *Angew. Chem. Int. Ed.*, 2023, **62**, e202216534; (e) X. Hao, Z. Tian, Z. Yao, T. Zang, S. Song, L. Lin, T. Qiao, L. Huang and H. Fu, *Angew. Chem. Int. Ed.*, 2024, **63**, e202410112; (f) Y. Wang, R.-P. Song, X.-Y. Li, W.-L. Chen, Y. Tian, S.-H. Zhang, Y.-D. Shao and D.-J. Cheng, *Org. Lett.*, 2024, **26**, 7161–7165; (g) Y.-D. Shao, D.-D. Han, H.-X. Jiang, X.-Y. Zhou, W.-K. Wang, J.-X. Zhang, Y.-F. Liu and D.-J. Cheng, *Org. Chem. Front.*, 2024, **11**, 3894–3899; (h) Pe. Zhang, B. Yuan, J. Li, C. Li, J. Guo, B. Zhang, G. Qu, H. Su, N. J. Turner and Z. Sun, *Angew. Chem. Int. Ed.*, 2025, **64**, e202416569; (i) Z.-H. Wang, H. Zhu, R.-X. Liu, Y.-X. Liu, X.-C. Liu and T.-Y. Lin, *Chin. J. Chem.*, 2025, **43**, 2929–2934; (j) W.-Q. Zheng, X.-X. Zhu, Z. Zhu, T. Yang, L. Zheng, R. Pan, S. Wang, L. Zhang, Q. Chen, J.-H. Xu, Y. Xie and G.-W. Zheng, *ACS Catal.*, 2025, **15**, 1522–1531; (k) Z. Yao, R. Meng, Z. Zhou, L. Yu, Z. Wu, L. Tang, T. Qiao, K. Li, L. Huang, D. Song and H. Fu, *J. Am. Chem. Soc.*, 2025, **147**, 40616–40625
14. (a) J. Feng, B. Li, Y. He and Z. Gu, *Angew. Chem. Int. Ed.*, 2016, **55**, 2186–2190; (b) J. D. Jolliffe, R. J. Armstrong and M. D. Smith, *Nat. Chem.*, 2017, **9**, 558–562; (c) S.-C. Zheng, S. Wu, Q. Zhou, L. W. Chung, L. Ye and B. Tan, *Nat. Commun.*, 2017, **8**, 15238; (d) S. Jia, Z. Chen, N. Zhang, Y. Tan, Y. Liu, J. Deng and H. Yan, *J. Am. Chem. Soc.*, 2018, **140**, 7056–7060; (e) C. Ma, F.-T. Sheng, H.-Q. Wang, S. Deng, Y.-C. Zhang, Y.-C. Jiao, W. Tan and F. Shi, *J. Am. Chem. Soc.*, 2020, **142**, 15686–15696; (f) L. Jin, P. Zhang, Y. Li, X. Yu and B.-F. Shi, *J. Am. Chem. Soc.*, 2021, **143**, 12335–12344; (g) J. Wang, X. Qi, X.-L. Min, W. Yi, P. Liu and Y. He, *J. Am. Chem. Soc.*, 2021, **143**, 10686–10694; (h) J. Feng and Z. Gu, *SynOpen.*, 2021, **5**, 68–85; (i) D. Ji, J. Jing, Y. Wang, Z. Qi, F. Wang, X. Zhang, Y. Wang and X. Li, *Chem.*, 2022, **8**, 3346–3362; (j) H. Liu, K. Li, S. Huang and H. Yan, *Angew. Chem. Int. Ed.*, 2022, **61**, e202117063; (k) S. Wu, S.-H. Xiang, J. K. Cheng and B. Tan, *Tetrahedron Chem.*, 2022, **1**, 100009; (l) B. Cai, Y. Cui, J. Zhou, Y.-B. Wang, L. Yang, B. Tan and J. Wang, *Angew. Chem. Int. Ed.*, 2023, **62**, e202215820; (m) W. Li, S. Chen, J. Xie, Z. Fan, K. Yang and Q. Song, *Nat. Synth.*, 2023, **2**, 140–151; (n) P.-F. Qian, T. Zhou and B.-F. Shi, *Chem. Commun.*, 2023, **59**, 12669–12684; (o) Z.-H. Li, Q.-Z. Li, H.-Y. Bai and S.-Y. Zhang, *Chem Catal.*, 2023, **3**, 100594; (p) L.-W. Zhan, C.-J. Lu, J. Feng and R.-R. Liu, *Angew. Chem. Int. Ed.*, 2023, **62**, e202312930; (q) J. Feng, C.-J. Lu and R.-R. Liu, *Acc. Chem. Res.*, 2023, **56**, 2537–2554; (r) S.-H. Xiang, W.-Y. Ding, Y.-B. Wang and B. Tan, *Nat. Catal.*, 2024, **7**, 483–498; (s) M. An, C.-J. Lu, F.-B. Ge, W.-G. Zhou, L.-W. Zhan, S. Zhang and R.-R. Liu, *ACS Catal.*, 2024, **14**, 13892–13902; (t) L.-L. Xi and R.-R. Liu, *Trends Chem.*, 2024, **6**, 556–571; (u) X. Ma, M. Tan, L. Li, Z. Zhong, P. Li, J. Liang and Q. Song, *Nat. Chem.*, 2024, **16**, 42–53; (v) Q.-H. Wu, M. Duan, Y. Chen, P. Yu, Y.-B. Wang, J. K. Cheng, S.-H. Xiang, K. N. Houk and B. Tan, *Nat. Catal.*, 2024, **7**, 185–194; (w) P. Wu, W.-T. Zhang, J.-X. Yang, X.-Y. Yu, S.-F. Ni, W. Tan and F. Shi, *Angew. Chem. Int. Ed.*, 2024, **63**, e202410581; (x) R. Mi, R. Wu, J. Jing, F. Wang, X.-X. Li, X. Hong and X. Li, *Sci. Adv.*, 2024, **10**, eadr4435; (y) C. Li, X.-W. Chen, L.-L. Liao, Y.-Y. Gui, J.-W. Yang, S. Zhang, J.-P. Yue, X. Zhou, J.-H. Ye, Y. Lan and D.-G. Yu, *Angew. Chem. Int. Ed.*, 2025, **64**, e202413305.

View Article Online
DOI: 10.1039/D6SC03274E

Data availability

The data supporting this article have been included as partof the supplementary information (SI). CCDC 2494773 contains the supplementary crystallographicdata for this paper.